

Heliostat Fatigue Loads

Proposal for Estimation of Wind Load Collectives

Andreas Pfahl¹ 

¹ German Aerospace Center (DLR), Institute of Solar Research, Solar Power Plant Technology, Germany

Abstract. An approach to estimate the wind load spectra for heliostats is proposed. It is based on the wind-induced fatigue cycle counts for buildings given by the Eurocode EN 1991 and considers heliostat specific impact factors. The approach can be further refined if data on specific wind and heliostat field properties are available.

Keywords: Point Focus Systems, Heliostats, Wind Loads, Fatigue

1. Introduction

The mean and peak wind loads on heliostats can be determined by means of wind tunnel tests [1] [2]. However, for economic dimensioning that excludes failure due to fatigue, the number of wind load cycles N_g at the various load levels, the so-called wind load spectrum, must be known as well.

The main reason for the load fluctuations is the turbulent characteristic of the wind. The wind load spectra of heliostats depend mainly on the following impact factors:

- Weibull distribution of the wind at site
- Distribution of the wind direction (wind rose)
- Wind speed profile
- Turbulence intensity profile
- Turbulent energy spectra
- Heliostat size/height
- Heliostat orientations during operation and at stow
- Heliostat position within heliostat field (wind shading)
- Dynamic load amplification due to resonance effects

Determining the wind load spectra for a specific site is rather complex. To determine the wind load cycles, extensive wind speed data are required and methods like the rainflow-counting algorithm have to be applied. But, often the needed data is not available. Therefore, a more general approach is desirable.

2. Method

As a simplified way to determine the wind load spectra, the Eurocode EN 1991 1-4, B.3 [3] gives wind-induced fatigue cycle counts for buildings (Figure 1, left). The loads are given in percentage of the maximum peak wind load event that occurs once within 50 years or with a

probability of 1/50 every year respectively. From the diagram it can be read e.g. that the total amount of counts of loads that are between 100% and 40% of that maximum 50 years load is 10^4 . According to the diagram, the total amount of counts of all wind load fluctuations is 10^9 .

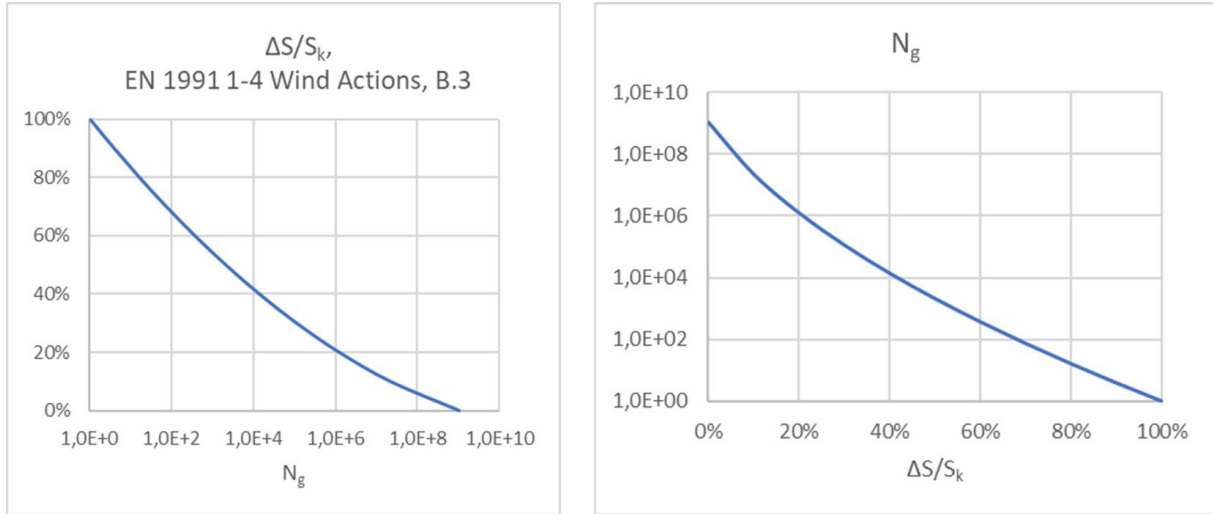


Figure 1. Wind load spectrum given by Eurocode EN 1991 1-4, B.3 [3] (left), transformed spectrum for easier adaption to heliostat specifics (right).

Holmes shows that the sensitivity of these load counts to wind climate and dynamic response is low [4]. That allows to use EN 1991 also to estimate the wind load spectra of heliostats. This assumption was confirmed by a study that determined the load spectra for a specific heliostat at a specific site [5]. It was based on the measured wind speed Weibull distribution of the site [6] (Figure 2, left) and on measured hinge moments which included dynamic response. The resulting stow load spectrum is similar to the one given by EN 1991 (Figure 1, left, and Figure 2, right).

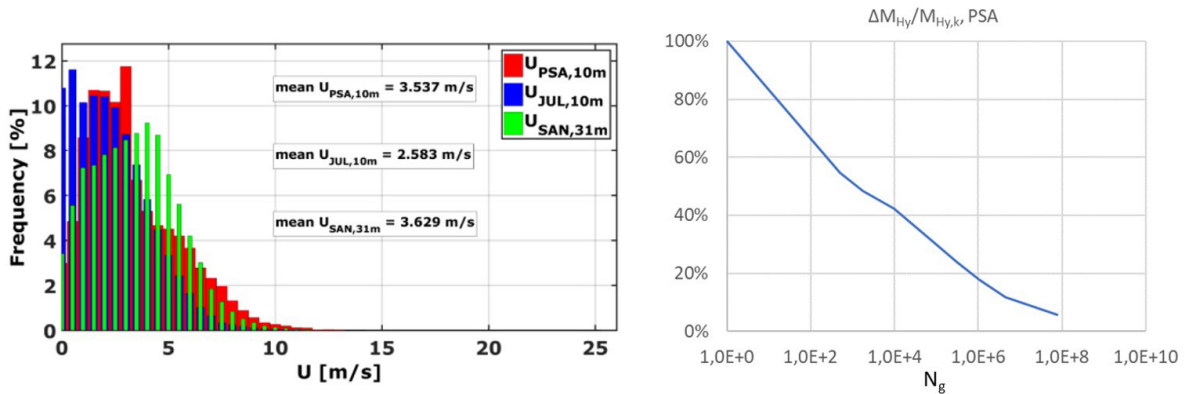


Figure 2. Weibull distribution of wind speed at three different locations [6] (left), stow hinge moment spectrum based on local wind speed distribution [5] (right).

3. Sample Case

For to be able to apply EN 1991 1-4, B.3, it must be adapted to the specifics of heliostat fields. Especially, it must be distinguished between the stow position with horizontal mirror and the orientations during operation. To explain the corresponding method, it is described in the following using a sample case. The counts for the drag force, the hinge moment, and the moment about the azimuth axis are determined for a heliostat that is at the edge of the field and therefore not wind shaded. The following data are assumed:

Heliostat dimensions

- Mirror height $h = 5 \text{ m}$
- Mirror width $b = 6 \text{ m}$
- Mirror area $A = 30 \text{ m}^2$
- Elevation axis height $H = 2.7 \text{ m}$

Wind properties

- Wind speed power law exponent $n = 0.15$
- Gust factor $R = 1.6$
- 50 years gust speed at 10 m height $V_{stow,peak,10m} = 45 \text{ m/s}$
- 50 years gust speed at height H $V_{stow,peak,H} = 37 \text{ m/s}$
- 50 years mean wind speed at H $V_{stow,mean,H} = 23 \text{ m/s}$
- Max. operational gust speed at 10 m $V_{op,peak,10m} = 15 \text{ m/s}$
- Max. operational gust speed at H $V_{op,peak,H} = 12 \text{ m/s}$
- Max. operational mean wind speed $V_{op,mean,H} = 7.7 \text{ m/s}$
- Air density $\rho = 1.25 \text{ kg/m}^3$

Wind load coefficients [7]

- Peak drag force coefficient for stow $C_{Fx,peak,stow} = 0.6$
- Peak drag force coefficient for operation $C_{Fx,peak,op} = 4.0$
- Hinge moment coefficient for stow $C_{MHy,peak,stow} = 0.2$
- Hinge moment coefficient operation $C_{MHy,peak,op} = 0.6$
- Azimuth moment coefficient for stow $C_{Mz,peak,stow} = 0.02$
- Azimuth moment coefficient operation $C_{Mz,peak,op} = 0.29$

Resulting wind loads

- Peak drag force stow $F_{x,peak,stow} = 5.9 \text{ kN}$
- Peak drag force operation $F_{x,peak,op} = 4.4 \text{ kN}$
- Drag force for horizontal mirror at v_{op} $F_{x,peak,stow,v_{op}} = 0.66 \text{ kN}$
- Drag force for vertical mirror at v_{stow} $F_{x,peak,op,v_{stow}} = 40 \text{ kN}$
- Peak hinge moment stow $M_{Hy,peak,stow} = 9.9 \text{ kNm}$
- Peak hinge moment operation $M_{Hy,peak,op} = 3.3 \text{ kNm}$
- Hinge moment for horizontal mirror at v_{op} $M_{Hy,peak,stow,v_{op}} = 0.22 \text{ kNm}$
- Hinge moment for vertical mirror at v_{stow} $M_{Hy,peak,op,v_{stow}} = 30 \text{ kNm}$
- Peak azimuth moment stow $M_{z,peak,stow} = 1.0 \text{ kNm}$
- Peak azimuth moment operation $M_{z,peak,op} = 1.6 \text{ kNm}$
- Azimuth moment for horizontal mirror at v_{op} $M_{z,peak,stow,v_{op}} = 0.11 \text{ kNm}$
- Azimuth moment for vertical mirror at v_{stow} $M_{z,peak,op,v_{stow}} = 14 \text{ kNm}$

4. Results

For the estimation of the drag force counts, the approach includes the following steps:

1. Transformation: For to be able to calculate the load counts at stow and in operation more easily, the EN 1991 spectrum is transformed from $\Delta S/S_k$ over N_g to N_g over $\Delta S/S_k$ (Figure 1, right).

2. Stow load counts: The maximum 50 years peak wind load $F_{x,peak,stow} = 5.9$ kN is calculated by using the 50 years wind speed event $v_{stow,peak,10m} = 45$ m/s given by standard wind load maps (e.g. [3], [8], [9]). This drag force occurs once every 50 years and is the upper limit of the abscissa of the graph in Figure 3, left. It is assumed that the heliostat is in stow position only for wind speeds above the operational wind speed. Therefore, there are no additional load counts for wind speeds below $v_{op,mean,H} = 7.7$ m/s which corresponds for a heliostat in stow position to a drag force of $F_{x,peak,stow,v_{op}} = 0.66$ kN (note the horizontal graph for drag forces up to this value).
3. Operation load counts: If the heliostat would not go to stow position but remained in upright position for all wind speeds, the drag force at the maximum 50-years wind speed would be $F_{x,peak,op,v_{stow}} = 40$ kN which would be the upper limit of the abscissa of the wind load spectrum. But, since the heliostat is in stow for wind speeds above the maximum operational wind speed, the counts start only for operational drag forces $F_{x,peak,op} = 4.4$ kN and is continued for lower values (Figure 3, middle).
4. Total load spectrum: The complete drag force spectrum is gained by just adding the stow load counts and the operational load counts (Figure 3, right). For loads above 4.4 kN, only stow loads occur while for loads below that value, almost only the operational loads are of impact because of the logarithmic scale.

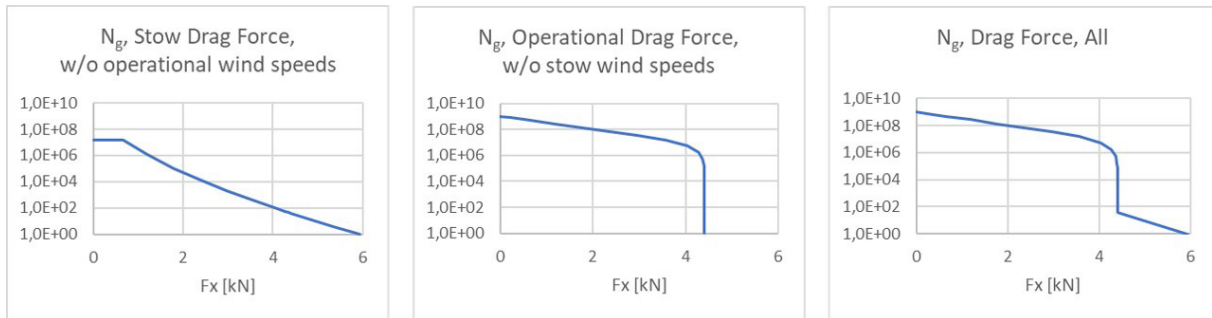


Figure 3. Drag force spectra: Stow (left), operation (middle), total (right). Both, stow and operation, is of impact on the total load counts.

The resulting wind load spectrum can be applied to test the fatigue resistance of a component. As an example, a heliostat component that is loaded by the drag force shall be tested. The load counts for drag forces above 4.4 kN are 40 and drag forces above 5.2 kN occur 5 times within 50 years. To be conservative and to keep the amount of test series low, the component could be loaded 40 times with 6 kN (which occurs only once in 50 years). Or, the component could be loaded e.g. 5 times with 6 kN and the remaining 35 times with only 5.2 kN which is less conservative but would mean 2 test series instead of 1. The operational wind load counts would have to be tested by applying 10^6 times 4.4 kN. More load cycles are not needed since steel components can be considered long-term resistant if they are able to resist a certain load level 10^6 times.

For the drag force, the maximum load in operation $F_{x,peak,op} = 4.4$ kN is 25% lower than the maximum stow load $F_{x,peak,stow} = 5.9$ kN. For that reason, stow loads and operational loads are both of significant impact on the shape of the total load spectrum (Figure 3). But, for the hinge moment, the maximum load in operation $M_{Hy,peak,op} = 3.3$ kNm (Figure 4, middle) is more than 60% lower than the maximum stow load $M_{Hy,peak,stow} = 9.9$ kNm (Figure 4, left). Therefore, the operational load counts are of only small impact on the total wind load spectrum (Figure 4, right).

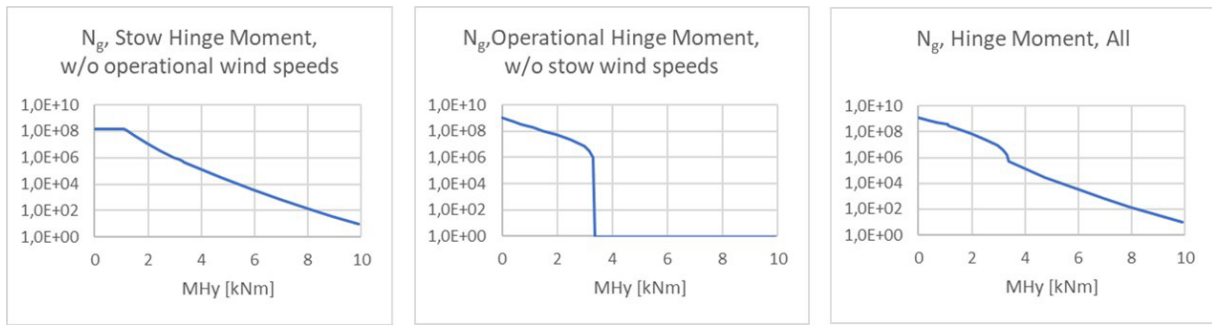


Figure 4. Hing moment spectra: Stow (left), operation (middle), total (right). The stow loads are of dominant impact on the shape of the total load spectrum.

For the hinge moment at stow, the vertical wind speed component is decisive. It fluctuates with an approximately ten times higher frequency than the longitudinal one [10]. Therefore, the stow load counts for the hinge moment are multiplied by ten. This leads to 10 times higher load counts (Figure 4, left and right).

When the heliostat is in horizontal stow position, the azimuth moment is very low because the area of attack of the concentrator is very small vertically to the azimuth axis. Therefore, the maximum operational load $M_{z,peak,op} = 1.6$ kNm (Figure 5, middle) is not lower but even 60% higher than the maximum load in stow $M_{z,peak,stow} = 1.0$ kNm (Figure 5, left). This results in a negligible impact of the stow loads on the total spectrum (Figure 5, right).

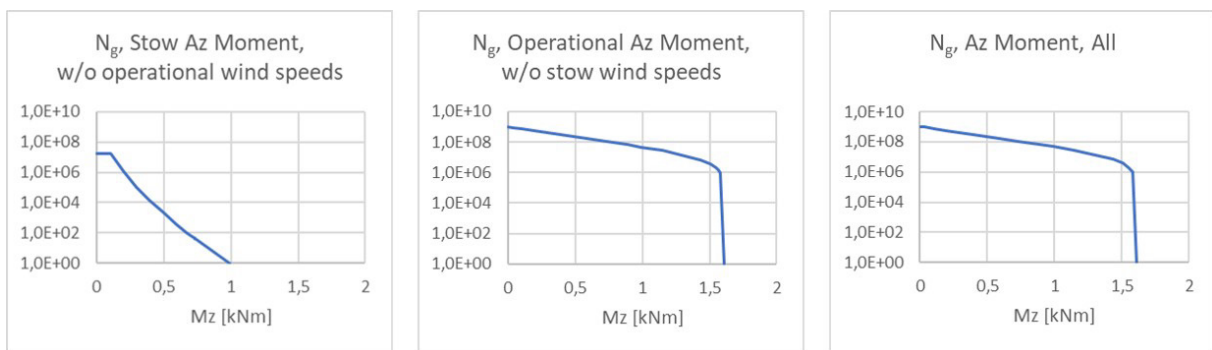


Figure 5. Azimuth moment spectra: Stow (left), operation (middle), total (right). Operation is dominant for the total load counts.

5. Summary and Outlook

With Eurocode EN 1991 1-4, B.3 [3], the wind load spectra for heliostats can be easily estimated. The shape of the spectra depends on the ratio of the storm wind speed to the maximum operational wind speed and on the ratio of the stow wind load coefficient to the operational wind load coefficient. The spectra enable to test the long-term fatigue durability of heliostat components.

The approach can be further refined and adapted to the specific wind and heliostat field properties:

- The most loaded heliostats are the ones at the edge of the heliostat field on the side of the prevailing wind direction (if no wind fence is foreseen). For other wind directions, these heliostats are wind shaded and the corresponding wind load counts could be subtracted.
- In this study, only the operational mirror orientation of highest wind load coefficient is assumed. But, it could be distinguished between different orientations. Spectra

for each orientation would have to be determined and to be added up to get the spectra of the total load counts.

- The load counts for 50 years can be adapted to the service life. So, if e.g. a service life of 30 years is assumed, the load counts can be multiplied by a factor of $30/50 = 0.6$.
- Here, it is assumed that the frequency of the vertical wind speed component is about 10 times higher than the longitudinal one. This factor can be determined more precisely taking the heliostat height into account.
- If the heliostat is in stow not only for wind speeds above the operational wind speed but e.g. generally at night, the operational load counts would have to be decreased while the stow load counts for these wind speeds would have to be increased.
- Dynamic load amplification at certain wind speeds due to resonance effects could also be considered if known.

Data availability statement

All relevant data is given in paragraph 3.

Author contributions

Andreas Pfahl: All.

Competing interests

No competing interests.

References

1. M. Emes, A. Jafari, A. Pfahl, J. Coventry, M. Arjomandi, "A Review of Static and Dynamic Heliostat Wind Loads," *Solar Energy* (225), 60-82, 2021, <https://doi.org/10.1016/j.solener.2021.07.014>.
2. A. Pfahl, "Wind Loads on Heliostats and Photovoltaic Trackers," PhD Thesis, DLR, TU Eindhoven, 2018, https://pure.tue.nl/ws/files/99010995/20180621_Pfahl.pdf.
3. British Standards Institution, "Eurocode 1 Actions on Structures – Part 1-4 General Actions – Wind Actions," BS EN 1991-1-4:2005.
4. J. Holmes, "Wind-Induced Fatigue Cycle Counts – Sensitivity to Wind Climate and Dynamic Response," In Vrag, Z. (ed), 7th ICCSM International Congress of Croatian Society of Mechanics, 2014, http://www.jdhconsult.com/index_htm_files/7ICCSM%20Wind-induced%20fatigue%20cycle%20counts%20sensitivity%20to%20wind%20climate%20and%20dynamic%20response.pdf.
5. A. Pfahl, K. Blume, N. Hanrieder, R. Uhlig, „MAHWIN – Teilvorhaben Winddatenanalyse, Freilandmessungen, Extremwertstatistik, Windlastkollektive, numerische Simulation,“ DLR-Schlussbericht zum BMWi-Projekt, 2020. <https://doi.org/10.2314/KXP:1778971571>.
6. N. Hanrieder, „MAHWIN – Grundlagen zur Bestimmung dynamischer Windlasten,“ DLR, 2017.
7. J.A. Peterka, R.G. Derickson, "Wind Load Design Methods for Ground Based Heliostats and Parabolic Dish Collectors," Report SAND92-7009, Sandia National Laboratories, Springfield, 1992. <https://www.osti.gov/servlets/purl/7105290>.
8. ASCE/SEI 7-22, "Minimum Design Loads and Associated Criteria for Buildings and Other Structures."

9. ATC Hazards by Location website, <https://hazards.atcouncil.org/#/>, accessed October 2023.
10. ESDU 85020, "Characteristics of Atmospheric Turbulence Near the Ground, Part II Single Point Data for Strong Winds (Neutral Atmosphere)," London, England, 1985.